Spatiotemporally Resolved Optical Measurements on Photocarrier Dynamics in Copper Monosulfide

Qing Miao,[a] Dawei He,[a] Xiuxiu Han,[a] Shengcai Hao,[a] Shuangyan Liu,[a] Jialu Fu,[a]

Yongsheng Wang,[*a] and Hui Zhao[b]*

[a] Key Laboratory of Luminescence and Optical Information, Ministry of education, Institute of Optoelectronic Technology, Beijing Jiaotong University, Beijing 100044, China.

[B] Department of Physics and Astronomy, The University of Kansas, Lawrence, Kansas 66045, USA.

ABSTRACT

In this paper, we report a transient absorption microscopy study of photocarrier dynamics in CuS crystals at room temperature. The photocarriers are injected in the sample by interband absorption of a 410 nm pump pulse and are detected by measuring the differential reflection of a 660 nm probe pulse as functions of both the time delay and the spatial position of the probe pulse. By analyzing the spatiotemporal dynamics of these carriers, we obtained a diffusion coefficient of 4.4 ± 0.5 cm^2 s^{-1}, which corresponds to a mobility of 163 cm^2 V^{-1} s^{-1}. The moderate photocarrier transport performance indicates potential optoelectronic applications of CuS as a semiconducting material. Our results also illustrate the prospects of fabricating two-dimensional materials and heterostructures with CuS.

1. INTRODUCTION

Copper monosulfide (CuS) is a layered semiconducting crystal with a room-temperature direct bandgap of about 2 eV.[1] It can be used in electronics,[2] mechanical devices,[3] and other fields. For example, CuS has been known for its essential role as a hole-transport layer[4] in solar cells[5] due to its low cost and outstanding photothermal performance. As a photocatalyst, CuS can help degrade organic pollutants and catalyze hydrogen production in water[6] owing to its remarkable optical properties and excellent photoelectric characteristics under visible light.[7] It is also know that CuS is difficult to dissolve in water and can oxidize in the air. It has a moderate thermal stability, with a decomposition temperature of about 220 °C.

The recent progress on studies of the two-dimensional (2D) materials based on layered crystals brings renewed interests to CuS, which is also a layered compound with a hexagonal lattice structure. It has been shown that the 2D semiconductors with hexagonal lattices can offer unique valley-selective optical coupling,[8–10] large binding energies of excitons, trions, and biexcitons,[11–14] and strong nonlinear optical responses[15–19] compared to their bulk counterparts. These characteristics have stimulated the efforts of applying them in electronic[20,21] and optoelectronic devices.[22–25] As such, it is interesting to explore CuS as a new potential material to fabricate 2D structures.

As a first step towards this goal, here we report a transient absorption study of photocarrier dynamics in CuS crystals. Understanding photocarrier dynamics is important for application of CuS in photocatalytic[26] and photovoltaic[27]. We time-resolve energy relaxation and recombination of photocarriers. Furthermore, the spatial resolution of the photocarrier dynamics allows us to observe the diffusion of the photocarriers and measure their diffusion coefficients. These results

provide basic understandings of the photocarrier dynamics in CuS and indicate the potential application of this material in 2D research.

2. EXPERIMENTAL

The bulk CuS crystals with high purity were acquired from 2D Semiconductors, INC. To obtain a sample for the optical measurements, we first remove the oxidized layers near the crystal surface by using an adhesive tape to cleave the sample, similar to the widely used mechanical exfoliation method.[37,38] Then, thick flakes of CuS are exfoliated from the fresh surface of the crystal and are transferred onto a polydimethylsiloxane (PDMS) substrate for inspection. After that, the selected flakes are transferred to a silicon substrate with a layer of 285 nm thermally growth SiO_2 for optical measurements.

Photocarrier dynamics is studied by a transient absorption technique.[39,40] We use a passively mode-locked Ti-doped sapphire laser to generate 100-fs pulses with a central wavelength of 820 nm and a repetition rate of 80 MHz. This pulse is divided into two parts by a beamsplitter. One part pumps an optical parametric oscillator (OPO), which has a signal output in the range of 490-750 nm. The other part of the pulse is sent to a beta barium borate (BBO) crystal to generate its second harmonic at 410 nm. The 410 nm pulse is focused on the sample by using an objective lens to a spot size of about 1.7 μm (in full width at half maximum), serving as the pump pulse to excite photocarriers in CuS. The probe pulse is obtained from the output of the OPO, which is focused on the sample by the same objective lens with a spot size of 1.8 μm. Considering the size of both spots, the spatial resolution of the system is about 2.5 μm. The reflected probe pulse from the sample is sent to one photodiode of a balanced detector. A portion of the probe pulse is taken before it enters the objective lens and is directly sent to the other photodiode of the balanced detector, which is used as the reference pulse for the balanced detection.

The purpose of using the balanced detection is to measure the differential reflection[41,42] of the signal from the sample with a high signal-to-noise ratio. The balanced detector outputs a voltage signal that is proportional to the difference of the average optical powers received by its two photodiodes. With the pump beam blocked, we adjust the power of the reference beam so that it matches precisely the power of the probe beam, so that the balanced detector output is zero volts. Once the pump is unblocked, the balanced detector outputs a voltage that is proportional to the differential reflection, which is defined as $\Delta R/R_0 = (R-R_0)/R_0$, where R and R_0 are the probe reflection with and without the pump reaching the sample, respectively. Since the probe power is nearly equally distributed to the two photodiodes, its common-mode noise (mostly the intensity noise) is also nearly evenly distributed. It is thus significantly suppressed by taking the difference. To further improve the signal-to-noise ratio, we use a mechanical chopper in the pump beam to modulate it at about 2 kHz. A lock-in amplifier measures the output voltage of the balanced detector at this frequency.

With this setup, the differential reflection signal can be measured as a function of the probe delay, which is the time difference between the probe and the pump pulses reaching the sample. The probe delay is controlled by changing the path length of the pump pulse by a linear motorized stage. The temporal resolution of the measurements is approximately 300 fs, since both pulses are about 200 fs at the sample, mainly due to the dispersion of the objective lens. To resolve the different reflection signals spatially, we scan the pump spot across the probe spot by changing the incident angle of the pump into the objective lens. All the measurements were performed at room temperature with the sample under ambient conditions.

Previously, various optical technologies have been used to study photocarrier diffusion [29] in semiconductors, such as transient gratings[30], spatially resolved pump-probe,[31] and spatially

resolved photoluminescence[32]. The spatially resolved pump-probe technique used here has been recently successfully applied to study the diffusion of excitons and electron-hole pairs in two-dimensional materials.[33-36]. The carrier mobility can also be inferred from the diffusion coefficient through the Einstein's relation.

3. RESULTS AND DISCUSSION

The crystal structure of CuS is shown in **Figure 1a**. It can be seen that CuS is a layered crystal with a hexagonal lattice. Since the atomic layers are connected by the weak van der Waals forces, it is possible to obtain thin layers and even single layers by exfoliation. This feature makes CuS a potential candidate to fabricate 2D materials and their heterostructures.

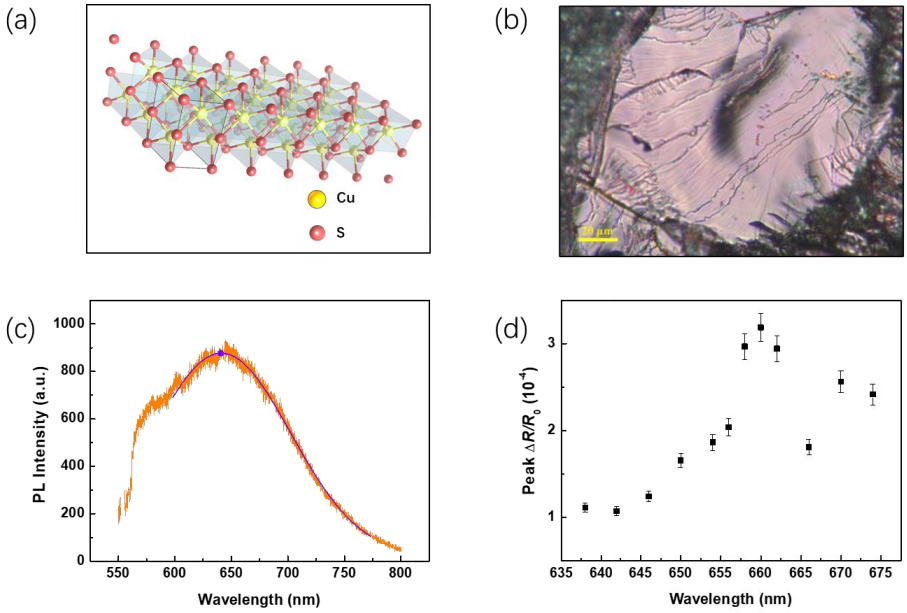

Figure 1. (a) The crystal structure of CuS. Gold and orange balls represent Cu and S atoms, respectively. (b) Optical microscope image of the bulk CuS crystal. The scale bar is 20 μm. (c) The orange curve shows the photoluminescence spectrum of the CuS flake under 532-nm and 4.5-mW continuous-wave laser excitation. The integration time is 30 s. The black curve is a fit to the spectrum, which gives a peak position of 636 nm. (d) Peak differential reflection signal from the CuS flake as a function of the probe wavelength. The sample was excited by a 410 nm pump pulse with an energy fluence of 16.7 μJ cm^{-2}.

One of the challenges of studying CuS is the sample degradation under ambient conditions. Hence, it is necessary to perform some preliminary treatments of the sample. It has been known that CuS undergoes a slow oxidation reaction in ambient conditions to produce copper monoxide (CuO), with the reaction equation as follows:

$$2\mathrm{CuS} + \mathrm{O_2} \rightarrow 2\mathrm{CuO} + 2\mathrm{S}. \quad (1)$$

Before making the flakes for the measurements, we treat the surface of the CuS crystal by peeling off the CuO on the surface. Because of its hard texture, CuS cannot be easily peeled off into a layered structure by the conventional mechanical exfoliation method. To solve this problem, at first, we anneal the CuS crystal. It is known that CuS decompose at 220 °C and rapidly oxidized with the following reaction equations,

$$2\mathrm{CuS} + 3\mathrm{O_2} \xrightarrow{\Delta} 2\mathrm{CuO} + 2\mathrm{SO_2}, \quad (2)$$

$$2\mathrm{CuS} \xrightarrow{220℃} \mathrm{Cu_2S} + \mathrm{S}. \quad (3)$$

We anneal the CuS crystal at 100 °C in a glove box and peel off its surface oxide layers while it is still hot. Then, after the crystal is cooled, we use a blade as a micro-surface eraser to obtain a high-quality CuS surface. The whole procedure is under an inert gas atmosphere to avoid oxidation reactions. An optical microscope image of the sample obtained with this procedure is shown in **Figure 1b**. To facilitate optical measurements, we transfer the sample to a Si/SiO_2 substrate (as described in Experimental).

Figure 1c shows the photoluminescence (PL) spectrum of the CuS sample, which is obtained under 532-nm continuous-wave laser excitation. The excitation power is 4.5 mW and the integration time is the 30 s. We observed a rather weak and broad PL peak center at about 636 nm with a width of about 200 nm. We are not aware of previously reported PL from CuS. To probe the origin of the PL, we performed transient absorption spectroscopy measurements. We obtained

the peak differential reflection signal as a function of the probe wavelength by choosing the probe delay that gives the maximum signal for each probe wavelength. The 410 nm pump excited the sample with a fluence of 16.7 μJ cm^{-2}. The results are shown in **Figure 1d**. We observed a peak at about 660 nm, which agrees well with the PL spectrum. Hence, both the PL and transient absorption spectroscopic measurements suggest a bandgap of about 1.88 eV, which is close to the previously reported bandgap of about 2 eV[1]. Based on these results, the PL could be attributed to the band-to-band allowed transition. The unusually broad spectrum could be due to the inhomogeneous broadening induced by shallow defects. However, further investigations, especially temperature-dependent PL spectroscopy, would be needed to fully understand the PL mechanism of CuS, which is beyond the scope of this study.

We next study the photocarrier dynamics in CuS. To ensure that the sample degradation under the laser radiation has minimal effects on the experimental results, each measurement was repeated immediately to confirm that the same result was obtained in such back-to-back scans. Furthermore, after one set of the measurements, we exposed the sample under the laser radiation with a high fluence of about 30 μJ cm^{-2} for 30 min. By repeating the measurement performed before such exposure, we confirm that the results are unchanged. These procedures ensure that the slow oxidation of the sample has minimal effects on the experimental results.

Figures 2a and **2b** show the differential reflection signals in long and short time ranges, respectively. The signals are obtained under the excitation of a 410 nm pump pulse with various energy fluences, as indicated in the caption, with a probe wavelength of 660 nm. We found that at each pump fluence, the signal has a sharp peak, characterized by a fast rise followed by a fast decay. After that, there is a small rise of the signal for about 10 ps, followed by a slow decay that persist for over 1 ns. To probe whether the photocarrier dynamics depends on the injected carrier

density, we plot the normalized data in **Figure 2c**. Clearly, the data measured with different pump fluences overlap well. Furthermore, we plot the signal at the peak, 100 ps, and 1 ns as a function of the pump fluence in **Figure 2d**. At each probe delay, the signal is proportional to the pump fluence. The results shown in Figures 2d and 2d thus indicate that the photocarrier dynamics is independent of the injected carrier density.

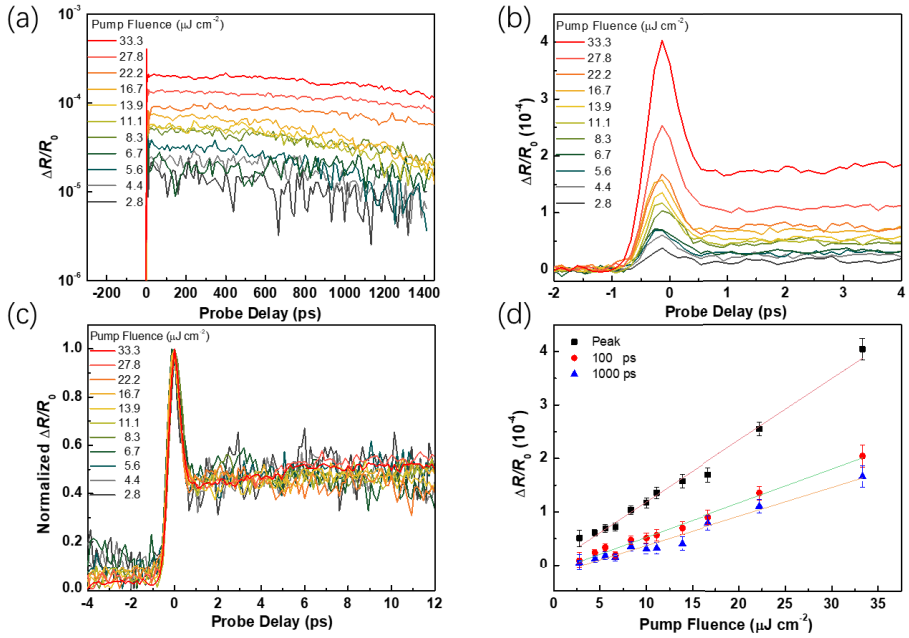

Figure 2. (a) The differential reflection signal from the CuS sample as a function of probe delay, measured with a 660-nm probe pulse and a 410-nm pump pulse with energy fluences of (from top to bottom) 33.3, 27.8, 22.2, 16.7, 13.9, 11.1, 8.3, 6.7, 5.6, 4.4, and 2.8 μJ cm^{-2}, respectively. (b) Similar to (a) but with a shorter time range near the zero probe delay. The black dashed curve is a Gaussian fit to the peak with a width of 350 fs. (c) Normalized signal shown in (b). (d) The differential reflection signal at the peak, 100 ps, and 1000 ps as a function of the pump fluence. The solid lines are linear fits.

To understand the features shown in Figure 2, we note that the 660-nm probe (1.88 eV) is tuned to the bandgap of CuS, while the 420-nm pump (2.95 eV) injects photocarriers, in the form of free electron-hole pairs, with high excess energy of several hundred meV. However, the peak signal was observed at a very early probe delay, suggesting that the hot carriers alter the bandedge

absorption instantaneously. To quantify the feature, we fit the peak near 0 delay with a Gaussian function, as shown as the dashed line in **Figure 2b**. The width of 350 fs is close to the pulse widths used in the study. From this observation, we could assign this peak to direct nonlinear interaction of the pump and probe pulses, such as sum-frequency generation or two-photon absorption. In that case, this feature would be unrelated to the photocarriers. One potential carrier-related origin could be due to defects in the sample that trapped carriers. However, in this case the peak height relative to the rest of the signal is expected to decrease with the pump fluence because with higher injected densities, a smaller fraction of the carriers would be lost to the traps.

The rest of the dynamics observed can be understood based on hot carrier energy relaxation and carrier recombination. Since the photocarriers are injected with several hundreds of meV above the bandedge, the energy relaxation of these hot carriers towards the bandedge states is expected to increase the population of carriers in the bandedge states, which are probed. Hence, the signal would increase. Based on the data, this energy relaxation process takes about 10 ps, and is independent of the carrier density. Finally, the decay of the signal is caused by loss of carrier population to the photocarrier recombination. Our data thus suggest a long photocarrier lifetime on the order of nanoseconds.

In order to study the transport properties of photocarriers in CuS, we next perform spatially resolved different reflection measurements. This is done by measuring the differential reflection signal as a function of probe delay and the probe position relative to the pump position. To achieve this, we move the pump spot across the probe spot and for each pump position we record the differential reflection signal as a function of the probe delay. This allows us to extract the Gaussian spatial distribution of the signal at various probe delays as shown in **Figure 3a**. A few examples of the profiles are shown in **Figure 3b** with probe delay of (from top to bottom) 5, 54, 108, and

145 ps, respectively. By fitting these profiles and those not shown in the figure by Gaussian functions (solid curves), we derive the width (full width at half maximum, FWHM) of each profile. The square width is plotted as a function of the probe delay in **Figure 3c**.

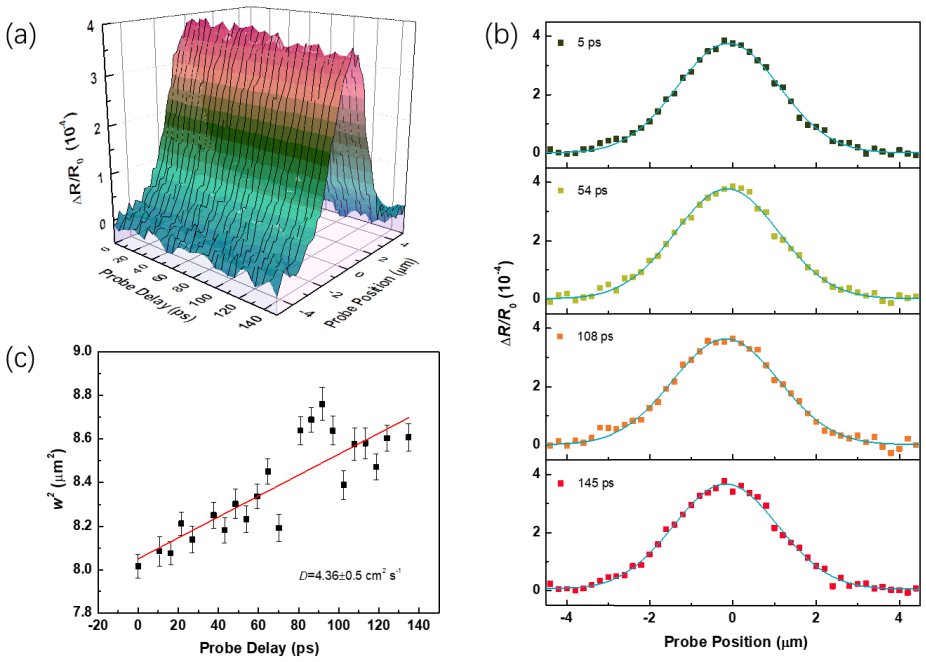

Figure 3. (a) The spatially resolved differential reflection signal from CuS measured with a 410-nm pump and a 660-nm probe as a function of probe delay and probe position. (b) A few examples of the spatial profiles. The probe delays are (from top to bottom) 5, 54, 108, and 145 ps, respectively. (c) The squared width of the spatial profile of the signal as a function of probe delay. The red line is a linear fit to the data points, which corresponds to a diffusion coefficient of 4.4 ± 0.5 cm^2 s^{-1}.

The measurement profile of the differential reflection signal is proportional to the photocarrier density profile, as confirmed in **Figure 2**. Hence, the observed broadening is due to photocarrier diffusion. By solving the diffusion compound equation, it can be shown that for the initial Gaussian distribution (defined by the pump spot), the profile remains a Gaussian distributions in the whole process,[44] and the width follows [45]

$$w^2(t) = w_0^2 + 11.09Dt, \quad (4)$$

where D and w_0 are photocarrier diffusion coefficients and the initial width. That is, the squared width (or the area covered by the photocarriers) increases linearly with time with a slope determined by the diffusion coefficient. By a linear fit as shown by the red line in **Figure 3c**, we obtained a diffusion coefficient of 4.4 ± 0.5 cm^2 s^{-1}. We note that, in order to further verify the experimental results, we repeated the spatially resolved pump-probe measurement on multiple locations of the sample and obtained reasonably consistent results. The uncertainty given reflects the spread of the results in these measurements. In the above analysis, we did not include the interlayer diffusion of carriers toward the surface. As a layered crystal, the interlayer carrier transport is expected to be much slower than the intralayer transport; and hence we expect a much smaller diffusion coefficient in the direction perpendicular to the sample surface.

Furthermore, by using the Einstein relation, $D/(k_BT)=\mu/e$, where k_B, e and T are the Boltzmann's constant, the elementary charge, and the lattice temperature (295 K), respectively, we obtain a carrier mobility of about 163 cm^2 $V^{-1}S^{-1}$. To our knowledge, the charge carrier mobility in CuS has not been measured previously.

4. CONCLUSIONS

We have studied photocarrier dynamics in CuS crystals by performed spatially, temporally, and spectrally resolved differential reflection measurements. The transient absorption and PL spectra established a direct bandgap of 1.88 eV for this material at room temperature. Time-resolved measurements show a hot carrier relaxation process of about 10 ps and a long photocarrier lifetime on the order of nanoseconds. The spatially and temporally resolved measurements revealed a photocarrier diffusion coefficient of about 4.4 cm^2 s^{-1} and a charge carrier mobility of about 163 $cm^2V^{-1}S^{-1}$. These results are important for understanding the optical properties of CuS.

Furthermore, its layered structure, long carrier lifetime, and moderate transport performances indicate that CuS could be a good candidate for developing new 2D materials and heterostructures.

AUTHOR INFORMATION

Corresponding Author

***E-mail: **yshwang@bjtu.edu.cn**

Notes

The authors declare no competing financial interest.

ACKNOWLEDGEMENT

We are grateful for the financial support of National Key R&D Program of China (2016 YFA0202302), National Natural Science Foundation of China (61527817, 61875236, 61905010, 61975007), Beijing Natural Science Foundation (Z190006), and U.S. National Science Foundation (DMR-1505852).

REFERENCES

(1) Yuan, K. D.; Wu, J. J.; Liu, M. L.; Zhang, L. L.; Huang, F. Q. Fabrication and microstructure of p-type transparent conducting CuS thin film and its application in dye-sensitized solar cell. *Appl. Phys. Lett.* **2008**, *93*, 132106-132100.

(2) Li, B.; Yi, X. Controllable Synthesis of CuS Nanostructures from Self-Assembled Precursors with Biomolecule Assistance. *J. Phys. Chem. C* **2007**, *111*, 12181-12187.

(3) Xu, J.; Cui, X. J.; Zhang, J.; Liang, H.; Wang, H.; Li, J. Preparation of CuS nanoparticles embedded in poly (vinyl alcohol) nanofibre via electrospinning. B. Mater. Sci. **2008**, *31*, 189-192.

(4) Ludwig, J.; An, L.; Pattengale, B.; Kong, Q.; Zhang, Xi.; Xi, P.; Huang, J. Ultrafast Hole Trapping and Relaxation Dynamics in p-Type CuS Nanodisks. *J. Phys. Chem. Lett*. **2015**, *6*, 2671.

(5) Li, J.; Jiu, T.; Tao, G. H.; Wang, G.; Sun, C.; Li, Fang, P.; J.; He, L. Manipulating surface ligands of copper sulfide nanocrystals: synthesis, characterization, and application to organic solar cells. *J. Colloid. Interf. Sci.* **2014**, *419*, 142-147.

(6) Bessekhouad, Y.; Robert, D.; Weber,J. V. Bi_2S_3/TiO_2 and CdS/TiO_2 heterojunctions as an available configuration for photocatalytic degradation of organic pollutant. *J. Photoch. Photobio. A.* **2004**, *163*, 569-580.

(7) Shen, X. P.; Zhao, H.; Shu, H.-Q.; Zhou, H.; Yuan, A.-H. Self-assembly of CuS nanoflakes into flower-like microspheres: Synthesis and characterization. *J. Phys. Chem. Solids* **2009**, *70*, 422-427.

(8) Mak, K. F.; He, K.; Jie, S.; Heinz, T. F. Control of valley polarization in monolayer MoS_2 by optical helicity. *Nat. Nanotechnol.* **2012**, *7*, 494-498.

(9) Xiao, D.; Liu, G. B.; Feng, W.; Xu, X.; Yao, W. Coupled spin and valley physics in monolayers of MoS_2 and other group-VI dichalcogenides. *Phys. Rev. Lett.* **2011**, *108*, 196802.

(10) Zeng, H.; Dai, J.; Yao, W.; Xiao, D.; Cui, X. Valley polarization in MoS_2 monolayers by optical pumping. *Nat. Nanotechnol.* **2012**, *7*, 490-493.

(11) Chernikov, A.; Berkelbach, T. C.; Hill, H. M.; Rigosi, A.; Li, Y.; Aslan, O. B.; Reichman, D. R.; Hybertsen, M. S.; Heinz, T. F. Exciton binding energy and nonhydrogenic Rydberg series in monolayer WS_2. *Phys. Rev. Lett.* **2014**, *113*, 076802.

(12) Kin, F.; Mak, K. F.; He, K.; Lee, C.; Lee, G. H.; Hone, J.; Heinz, T. F.; Jie,S. Tightly bound trions in monolayer MoS_2. *Nat. Mater.* **2013**, *12*, 207-211.

(13) Jones, A. M.; Yu, H.; Ghimire, N. J.; Wu, S.; Aivazian, G.; Ross, J. S.; Zhao, B.; Yan, J.; Mandrus, D. G.; Xiao, D. Optical generation of excitonic valley coherence in monolayer WSe_2. *Nat. Nanotechnol.* **2013**, *8*, 634-638.

(14) He, K.; Kumar, N.; Zhao, L.; Wang, Z.; Mak, K. F.; Zhao, H.; Shan, J. Tightly bound excitons in monolayer WSe_2. *Phys. Rev. Lett.* **2014**,*2*, 113-115,

(15) Zeng, H.; Liu, G. B.; Dai, J.; Yan, Y.; Zhu, B.; He, R.; Xie, L.; Xu, S.; Chen, X.; Yao, W. Optical signature of symmetry variations and spin-valley coupling in atomically thin tungsten dichalcogenides. *Sci. Rep-UK* **2013**, *3*, 1608.

(16) Song, Q. J.; Tan, Q. H.; Zhang, X.; Wu, J. B.; Sheng, B. W.; Wan, Y.; Wang, X. Q.; Dai, L.; Tan, P. H. Physical origin of Davydov splitting and resonant Raman spectroscopy of Davydov components in multilayer $MoTe_2$. *Phys. Rev. B* **2016**, *93*, 115409.

(17) Malard, L. M.; Alencar, T. V.; Barboza, A. P. M.; Mak, K. F.; Paula, A. M. D. Observation of intense second harmonic generation from MoS_2 atomic crystals. *Phys. Rev. B* **2013**, *87*, 201401(R).

(18) Li, Y.; Rao, Y.; Mak, K. F.; You, Y.; Wang, S.; Dean, C. R.; Heinz, T. F. Probing symmetry properties of few-layer MoS_2 and h-BN by optical second-harmonic generation. *Nano. Lett.* **2013**, *13*, 3329-3333.

(19) Yin, X.; Ye, Z.; Chenet, D. A.; Ye, Y.; O'Brien, K.; Hone, J. C.; Zhang, X. Edge nonlinear optics on a MoS_2 atomic monolayer. *Science* **2014**, *344*, 488-490.

(20) Radisavljevic, B.; Radenovic, A.; Brivio, J.; Giacometti, V.; Kis, A. Single-layer MoS_2 transistors. *Nat. Nanotechnol.* **2011**, *6*, 147-150.

(21) Radisavljevic, B.; Whitwick, M. B.; Kis, A. Integrated circuits and logic operations based on single-layer MoS_2. *Acs Nano* **2011**, *5*, 9934-9938.

(22) Wi, S.; Chen, M.; Da, L.; Nam, H.; Meyhofer, E.; Liang, X. Photovoltaic response in pristine WSe_2 layers modulated by metal-induced surface-charge-transfer doping. *Appl. Phys. Lett.* **2015**, *107*, 952-958.

(23) Baugher, B. W.; Churchill, H. O.; Yang, Y.; Jarilloherrero, P. Intrinsic electronic transport properties of high-quality monolayer and bilayer MoS_2. *Nano. Lett.* **2013**, *13*, 4212-4216.

(24) Yu, S. H.; Lee, Y.; Jang, S. K.; Kang, J.; Jeon, J.; Lee, C.; Lee, J. Y.; Kim, H.; Hwang, E.; Lee,S. Dye-Sensitized MoS_2 Photodetector with Enhanced Spectral Photoresponse. *Acs Nano* **2014**, *8*, 8285-8291.

(25) Cui, Q.; He, J.; Bellus, M. Z.; Mirzokarimov, M.; Hofmann, T.; Chiu, H. Y.; Antonik, M.; He, D.; Wang, Y.; Zhao, H. Transient Absorption Measurements on Anisotropic Monolayer ReS_2. *Small* **2015**, *11*, 5565-5571.

(26) Basu, M.; Sinha, A. K.; Pradhan, M.; Sarkar, S.; Negishi, Y.; Pal, T. Evolution of hierarchical hexagonal stacked plates of CuS from liquid-liquid interface and its photocatalytic application for oxidative degradation of different dyes under indoor lighting. *Environ. Sci. Technol.* **2010**, *44*, 6313-6318.

(27) Zhang, Y.; Tian, J.; Li, H.; Wang, L.; Qin, X.; Asiri, A. M.; Abdulrahman, O.; Sun, X. Biomolecule-assisted, environmentally friendly, one-pot synthesis of CuS/reduced graphene oxide nanocomposites with enhanced photocatalytic performance. *Langmuir* **2012**, *28*, 12893.

(28) Ramasamy, K.; Malik, M. A.; Revaprasadu, N.; O'Brien, P. ChemInform Abstract: Routes to Nanostructured Inorganic Materials with Potential for Solar Energy Applications. *Cheminform* **2013**, *44*, 3551-3569.

(29) Zhu, T.; Snaider, J. M.; Yuan, L.; Huang, L. Ultrafast Dynamic Microscopy of Carrier and Exciton Transport. *Annu. Rev. Phys. Chem.* **2019**. 70:219-244

(30) Hegarty, J.; Goldner, L.; Sturge, M. D. Localized and delocalized two-dimensional excitons in GaAs-AlGaAs multiple-quantum-well structures. *Phys. Rev. B* **1984**,30, 7346

(31) Smith, L. M.; Wake, D. R.; Wolfe, J. P.; Levi, D.; Klein, M. V.; Klem, J.; Henderson, T.; Morkoç, H. S.; Picosecond imaging of photoexcited carriers in quantum wells: Anomalous lateral confinement at high densities[J]. *Phys. Rev. B* **1988**, 38(8):5788-5791.

(32) Hillmer, H.; Hansmann, S.; Forchel, A.; Morohashi, M.; Lopez, E.; Meier, H. P.; Two-dimensional exciton transport in GaAs/GaAIAS quantum wells. *Appl. Phys. Lett.* **1988** 53(20), 1937.

(33) He, J.; He, D.; Wang, Y.; Cui, Q.; Ceballos, F.; Zhao, H. Spatiotemporal Dynamics of Excitons in Monolayer and Bulk WS_2. *Nanoscale* **2015**,7, 9526-9531.

(34) Liu, S.; Tan, C.; He, D.; Wang,Y.; Peng,H.; Zhao,H. Optical Properties and Photocarrier Dynamics of Bi_2O_2Se Monolayer and Nanoplates. *Adv. Opt. Mater.* **2020**, 8, 1901567 .

(35) Pan, S.; Kong, W.; Liu, J.; Ge, X.; Zhao, H.; Understanding Spatiotemporal Photocarrier Dynamics in Monolayer and Bulk $MoTe_2$ for Optimized Optoelectronic Devices. *ACS Appl. Nano Mater.* **2019**, 2, 459-464.

(36) Fu, Y.; He, D.; He, J.; Bian, A.; Zhao, H. Effect of dielectric environment on excitonic dynamics in monolayer WS_2. Adv. Mater. *Interfaces* **2019**, 6, 190137

(37) Novoselov, K. S.; Geim, A. K.; Morozov, S. V.; Jiang, D.; Zhang, Y.; Dubonos, S.V.; Grigorieva, I.V.; Firsov, A.A. Electric Field Effect in Atomically Thin Carbon Films. *Science* **2004**, 306(5696):666-669.

(38) Yuan,L.; Huang, L. Exciton Dynamics and Annihilation in WS_2 2D Semiconductors *Nanoscale* **2015**, 7(16):7402-7408.

(39) Wang, R.; Ruzicka, B. A.; Kumar, N.; Bellus, M. Z.; Chiu, H. Y.; Zhao, H. Ultrafast and spatially resolved studies of charge carriers in atomically thin molybdenum disulfide. *Phys. Rev.* **2012**, 86(4):p.045406.1-045406.5.

(40) Cui, Q.; Ceballos, F.; Kumar, N.; Zhao, H. Transient Absorption Microscopy of Monolayer and Bulk WSe_2. *Acs Nano* **2014**,8(3):2970-2976.

(41) Mcintyre, J. D. E.; Aspnes, D. E.; Differential reflection spectroscopy of very thin surface films. *Surf. Sci.* **1971**, 24(2):417-434.

(42) Axe, J. D.; Hammer, R.; Electroreflectance Spectra due to Free Carriers in Semiconductors. *J. Phys. Rev*. **1967**, 162(3):700-702.

(43) Ceballos, F.; Zhao, H. Ultrafast Laser Spectroscopy of Two-Dimensional Materials Beyond Graphene. *Adv. Funct. Mater.* **2016**, *27*, 1604509.

(44) Neamen, D. A. *Semiconductor physics and devices: basic principles;* McGraw-Hill: New York, America, 2012.